A new test method for obtaining stable mode III crack growth under RCF condition

S. Beretta, S. Foletti, M.G. Tarantino, K. Valliulin

Politecnico di Milano, Department of Mechanical Engineering., Via La Masa 34, 20156 Milano

ABSTRACT. *A novel experimental method has been developed in order to promote mode III co-planar crack propagation. Multiaxial out of phase fatigue tests have been carried out on two different steels on micro-notched specimens adopting a stress history typical of subsurface RCF. Three defect sizes, expressed in terms of Murakami's √area parameter, equal to 631 μm, 314 μm and 221 μm have been considered. In both materials the data clearly show that the threshold conditions for out of phase tests is lower than in simple torsional tests, moreover the shear growth is promoted. The main feature of the out of phase tests is that crack growth is accompanied plastic deformation and rubbing of cracks lips.*

INTRODUCTION

Mode III fatigue crack behaviour have been investigated by some researchers in order to better understand the complex mechanism of crack path under this loading condition [1]. Both turbine-generator shafts under transient torsional loading and components under rolling contact fatigue, (such as bearings, gears, rails and etc), exhibit mode III crack propagation [2].

The experimental investigations have shown that the mode III crack growth in a circumferentially notched shaft [3] could be very tortuous, resulting in a crack front rotation and segmentation often called factory roof crack surface. Tschegg experiments [4] revealed that there is a critical applied stress intensity factor value under which mode III crack propagation is no more stable, resulting in a mode I branching. According to Tschegg, this nominal value of the applied ΔK_{III} can be interpreted as a mode III fatigue threshold since the fracture mode changes from a macroscopically flat (mode III) to a factory roof (mode I) type. Moreover Nayeb-Hashemi et al [5] observed that a superimposed static axial load on the fatigue in torsion can promote stable mode III crack growth, since it reduces the sliding mode crack growth effect.

More recently different authors have obtained new experimental data for Mode II/Mode III [6, 7] propagation under the implicit assumption that the growth rate under RCF conditions can be obtained combining the experimental trend (threshold, growth rate) together with SIF calculations under the out-of-phase combination of Mode I + Mode II (see the discussion by Murakami [1] for application to 'shelling' railway failures). However, up to now there have not been attempts to verify the effective growth rate

under subsurface RCF conditions and to compare it with data under simple torsion, while only 'experimentally derived' shear growth data on small defects have been incorporated into RCF models for subsurface fatigue [8-9].
The aim of the present study is to present a new experimental method in order to promote mode III co-planar crack propagation under mixed-mode loading conditions representing subsurface RCF conditions. The novelty of the method consists in out-of-phase multiaxial fatigue tests onto specimens containing micro-notches that were previously subjected to Mode I precracking at R=-2. The results for two different steels show that the presence of a superimposed compression enhances the shear coplanar growth resulting in $\Delta K_{th,III}$ values much lower than the threshold condition for simple torsion. This enhanced damage mechanism, that cannot be described neither in terms of fatigue criteria nor in terms of crack driving force at the crack tip, is characterized by intense plastic deformation and rubbing of crack lips with an opening of the crack faces.

EXPERIMENTAL DETAILS

Materials

The materials analyzed are a gear steel (SAE 5135) and a bearing steel. First of all, the basic properties as well as the fatigue behaviour of the two materials were determined. Table 1 summarizes the Vickers micro-hardness average value measurement (load 0.98N) and the results of monotonic and cyclic tests. Both the two materials showed a strain hardening behaviour when subjected to cyclic loading.

Table 1. Materials mechanical properties

	HV	UTS [MPa]	σ_y [MPa]	$\sigma_{y,cyclic}$ 0.2% [MPa]
SAE 5135 gear steel	550	2150	1395	1735
Bearing steel	600	2364	1982	2072

Specimens and preparation

Multiaxial fatigue tests were carried out on pre-cracked micro-notched hourglass specimens. Three defect sizes, expressed in terms of Murakami's √area parameter, equal to 631 μm, 314 μm and 221 μm have been considered. The geometry of the specimens and micro-notches adopted are presented in Figure 1.
Before starting multiaxial fatigue tests, all specimens were electro polished to avoid the effect of the surface residual stresses. Then, artificial micro notches were introduced by means of electro-discharging machining (EDM). In order to promote co-planar crack propagation, a preliminary Mode I fatigue test pre-cracking procedure was adopted. For the gear steel all specimens were subjected to bending fatigue for 1.2×10^7 cycles at R=-2 at a stress levels very close to $\Delta K_{th,I}$. For the bearing steel all specimens were subject to push-pull axial fatigue for 1.0×10^7 cycles at R=-2 at a stress level close to $\Delta K_{I,th}$ till $N_f=10^7$.

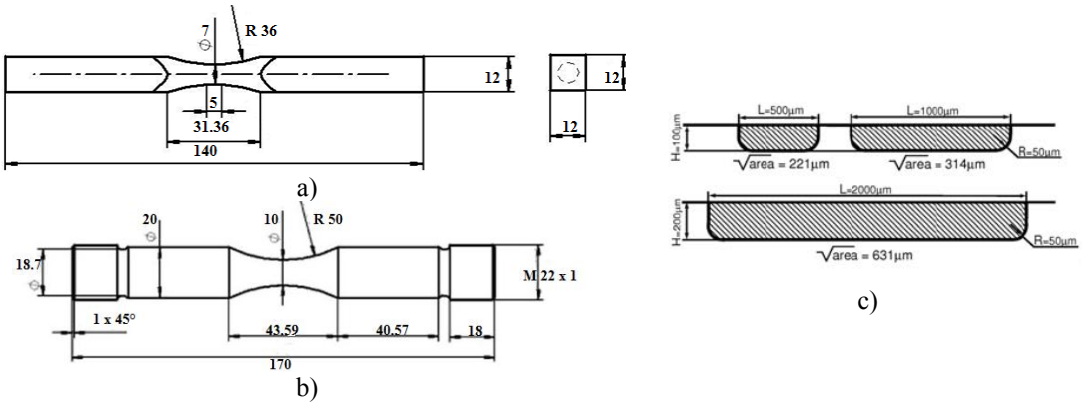

Figure 1. Out-of phase fatigue tests: a) gear steel specimen geometry, b) bearing steel specimen geometry, c) micro-notches used

Pre-cracking procedure induced small non-propagating cracks at the bottom of the notch with a depth of approximately 20 µm. All specimens were observed under SEM for verifying the success of pre-cracking procedure (if not successful the Mode I loading was repeated).

Multiaxial Fatigue Tests

Multiaxial fatigue tests were conducted in force/torque control by means of a MTS 809 Axial Torsional System. In order to simulate the most detrimental subsurface stress in rolling contact fatigue problems, the adopted loading path is characterized by an axial force always in compression and shifted on 90◦ degrees relatively to the torsional cycle, moreover the ratio between the normal mean stress and shear stress amplitude is approximately equal to 1.5 (typical for subsurface position where τ_{max} is present) [10] (Figure 2).

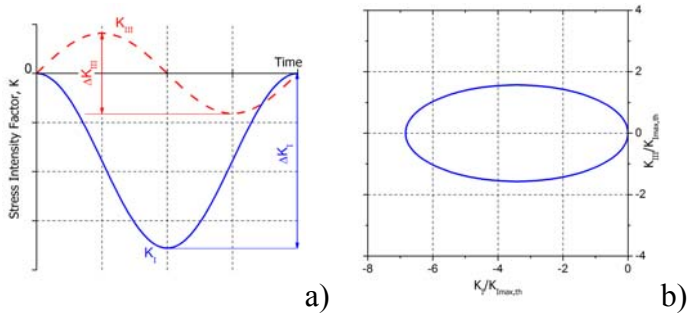

Figure 2. Load pattern scheme adopted for fatigue testing: a) in terms of stress intensity factor, b) normalized by $K_{Imax,th}$

The main idea of the experimental onset is to run fatigue tests decreasing the load from one specimen to another till no fatigue crack growth will occur. During the fatigue tests

an optical microscope Leica system permitted to control surface mixed-mode crack advance continuously during the test. After the fatigue test, cryogenic static rupture with further examination by SEM permitted to estimate in side propagation type and its order. After the tests all the specimens were examined under SEM in order to observe the specimen surface and, after static criogenic rupture, the fracture surface.

MULTIAXIAL FATIGUE TEST RESULTS

Gear steel

Out of phase fatigue test results carried out on the gear steel are shown in the Figure 3.

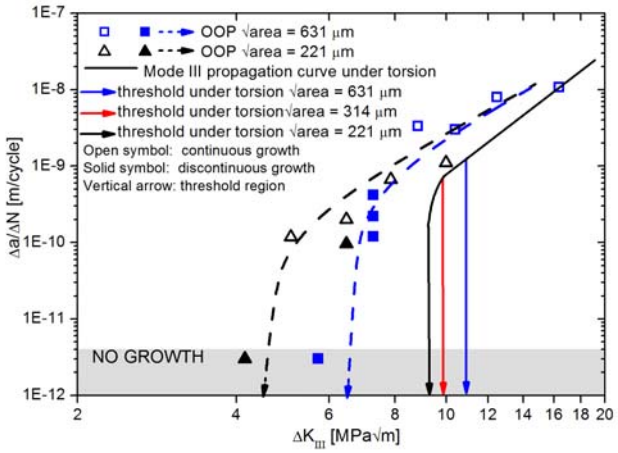

Figure 3. Coplanar Mode III average propagation rates: multiaxial fatigue test v.s. pure torsional fatigue tests results, in terms of ΔK_{III} (gear steel)

Previous results obtained by the authors [11-12] on the same steel showed that in pure torsion $\Delta K_{th,III}$ is approximately equal to the Mode I threshold for defects with √area< 1000 μm. Having a look at the results of the multiaxial fatigue tests is it clear that the out-of-phase scheme of loading promotes Mode III co-planar crack growth ,since it was possible to obtain continuous Mode III propagation at ΔK_{III} levels much lower than Mode I threshold, and inhibits the development of Mode I kinked cracks. In particular, it is possible to observe that in the tests where $\Delta K_{III}<\Delta K_{I,th}$ no appreciable surface growth could be observed (Figure 4), while in all tests at $\Delta K_{III}>\Delta K_{I,th}$ there is the development of mode I tilted cracks along the crack front (Figure 5).

This 'enhanced propagation' respect to simple shear stress is also confirmed by the stability of the growth rate that can be observed in Figure 6. In order to estimate Mode III co-planar crack growth speed under out-of-phase loading, three out-of-phase fatigue test at the same stress levels, $\Delta K_{III}/\Delta K_{th,I}=1.08$, were carried out , interrupting the test at different number of test cycles, and breaking them in liquid nitrogen to measure the depth of the crack (see Figure 6). The growth rate remains stable with a 400 μm crack advance (see Figure 6d), while in Mode II/Mode III experiments the crack tend stop

after a short propagation (some tenths of microns) because of the development of a significant friction along the crack faces [12-15].

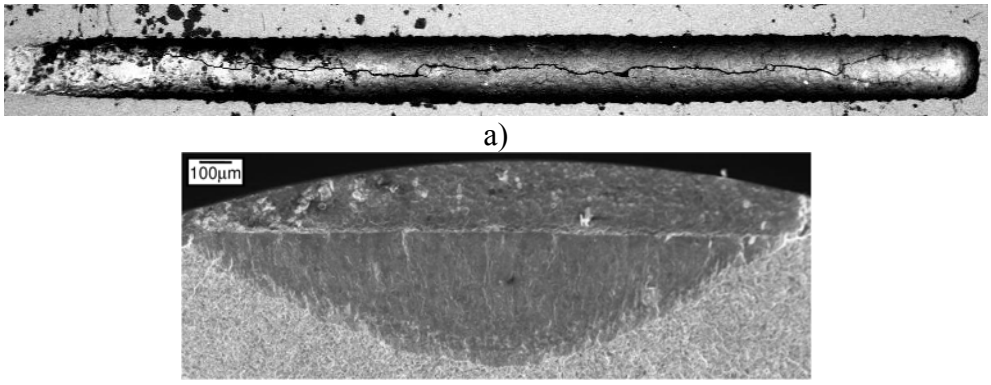

a)

b)

Figure 4. OOP fatigue test fractography; specimen tested at $\Delta K_{III}=0.85\Delta K_{th,I}$ test interrupted at $N_f= 1.2\cdot10^5$ cycles: a) specimen surface; b) 90°tilted view, coplanar Mode III crack, 400µm deep.

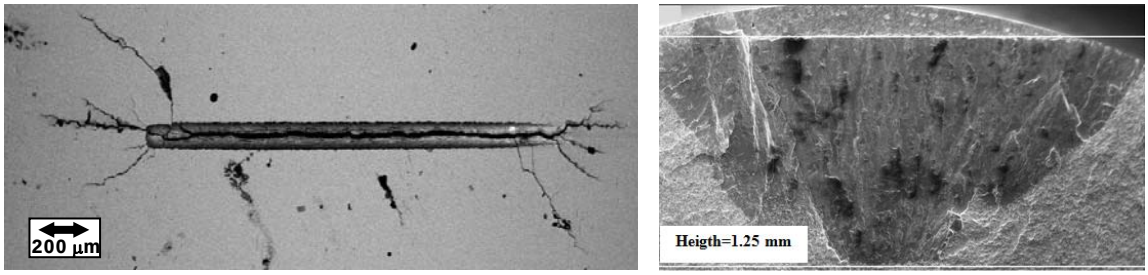

a) b)

Figure 5. OOP fatigue test fractography; specimen tested at $\Delta K_{III}=1.2\Delta K_{th,I}$ test interrupted at $N_f= 1.2\cdot10^5$ cycles: a) surface mix-mode cracks top view; b) specimen after static cryogenic rupture 90◦ tilted view, coplanar Mode III crack 1250µm deep.

This ‘promotion of shear growth’ under OOP conditions is a challenge to our common understanding based on LEFM since the application of a compressive Mode I should enhance the effect of friction [12, 1, 13, 16]. A possible reason of coplanar growth stability is the evidence of huge plastic deformation and rubbing of fracture lips. As it can bee seen from Figure 7, the crack after out-of-phase fatigue test remains widely open in comparison with the state after pre-cracking. This crack rubbing/deformation could promote shear propagation since it prevents the friction of the crack faces. However, a simple LEFM model is not able to describe this kind of material damage.

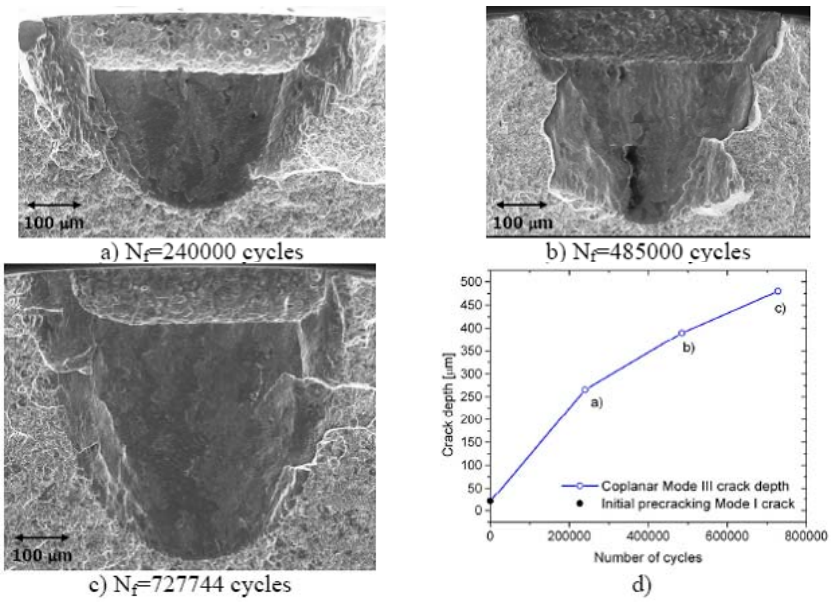

Figure 6. Mode III co-planar continuous growth for micronotch √area = 221.2µm at $\Delta K_{III}=1.08\Delta K_{th,I}$ with tests interrupted at different number of cycles: a) specimen crack depth 265 µm, b) specimen crack depth 390 µm; c) specimen crack depth 480 µm; d) co-planar crack depth vs. cycles.

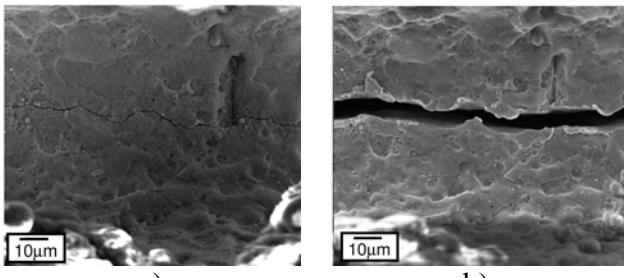

Figure 7. Evidence of crack lips opening for specimen tested at $\Delta K_{III}=\Delta K_{th,I}$: a) pre-crack; b) after OOP test.

Bearing steel

Out of phase fatigue test results carried out on a bearing steel are shown in Figure 8 (due to confidentiality issues, experimental results are presented in normalised form, with ΔK_{III} normalised respect to the $\Delta K_{Ith,LC}$ for long cracks). As well as for the gear steel, all OOP tests results showed a stable shear co-planar Mode III propagation.

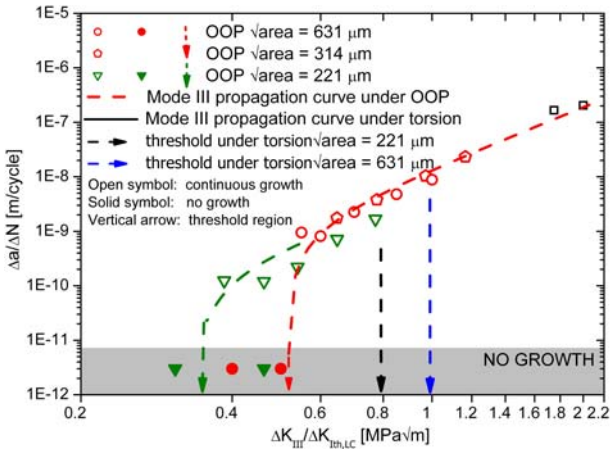

Figure 8. Coplanar Mode III average propagation rates: multiaxial fatigue test v.s. pure torsional fatigue tests results, in terms of ΔK_{III} (bearing steel)

During multiaxial fatigue testing an evidence of continuous debris emission from a pre-cracks has been observed (also for non-propagating cracks). Micro pre-cracks surface observations after the fatigue test showed that the cracks lips remain open (Figure 9).

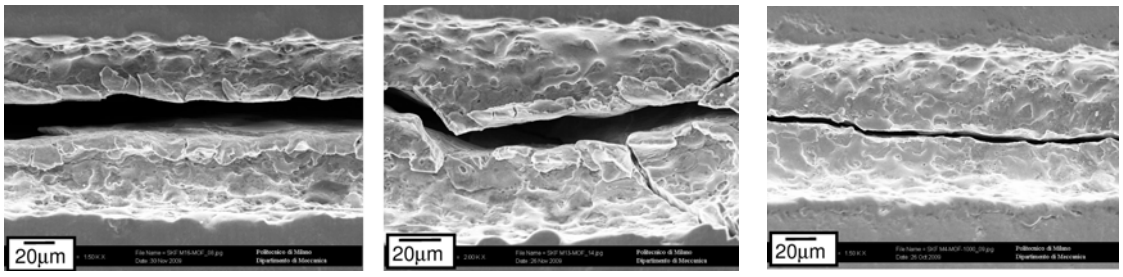

a) b) c)

Figure 9. Evidence of crack lips opening : a) specimen tested at ΔK_{III}=1.3 $\Delta K_{th,I}$; b) specimen tested at ΔK_{III}=1.1 $\Delta K_{th,I}$; c) specimen tested at ΔK_{III}=0.7 $\Delta K_{th,I}$

Sectioning on a specimen tested at ΔK_{III}=0.8 $\Delta K_{th,I}$ (test interrupted at $N_f = 2 \cdot 10^5$ cycles) showed that the crack opening is constant within the whole coplanar crack depth (Figure10). The crack fracture surface opening is almost 18 μm.
Surface fracture fractographies on the sectioned specimen also highlighted the typical appearance of a crack under RCF loading condition (Figure 10b), several sub-surface multiple sites of crack branching have also been observed at the main co-planar crack propagation pattern. The RCF crack appearance shows evidence of material intense deformation under the local rubbing and sliding phenomenon.

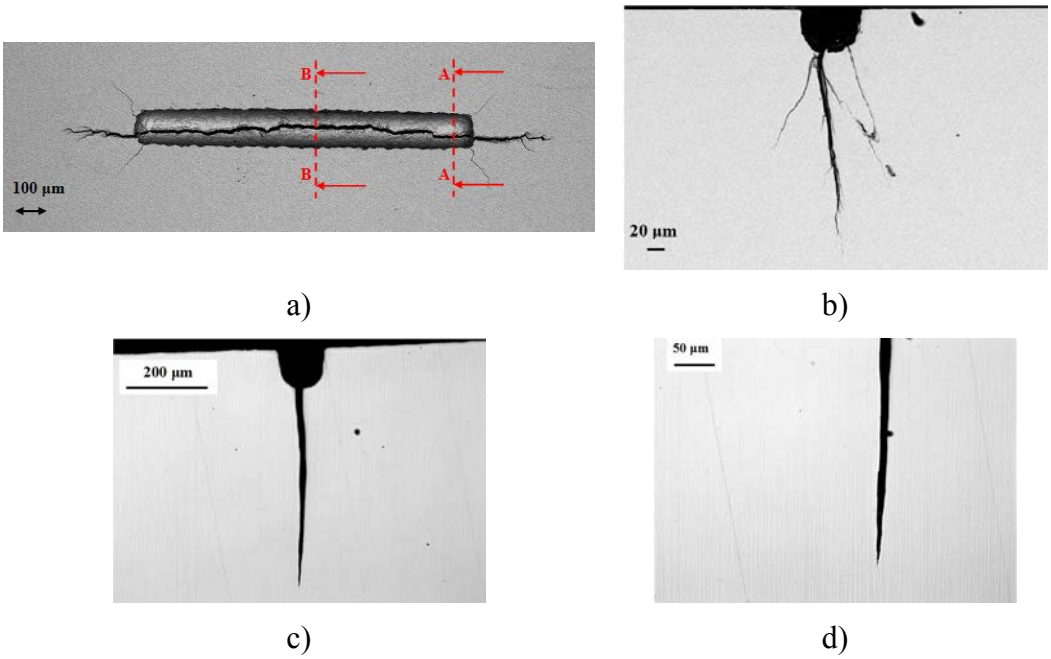

Figure 10. OOP fatigue specimen tested at $\Delta K_{III}=0.8\Delta K_{th,I}$ test interrupted at $N_f=2\cdot10^5$ cycles: a) specimen surface; b) typical appearance of a RCF crack; c) central area section; d) magnification

DISCUSSION

Application of multiaxial fatigue criteria

In order to predict the "peculiar" experimentally observed near-threshold fatigue crack behaviour, different multiaxial fatigue criteria have been applied. The axial and torsion fatigue limits, σ_w and τ_w respectively, of micro-notched specimens have been experimentally obtained (for both the bearing and the gear material the ratio σ_w/τ_w is less than one).
Different integral and critical plane stress type multiaxial fatigue criteria have been applied. The multiaxial fatigue criteria are reported in Table 1.
Due to the experimental obtained ratio $\sigma_w/\tau_w<1$ the Findley and the Liu-Zenner criterion cannot be applied since the criteria material constants are not defined.
In order to predict the near-threshold fatigue crack behaviour, the criteria have been applied to experimental data where coplanar crack growth has been observed as well as to specimens which had no evidence of mode III propagation.
The prediction error can be defined in the following way:

$$\text{error} = \frac{\sigma_{eq} - \sigma_{\lim}}{\sigma_{\lim}} \cdot 100\%$$

As it can be observed from Figure 11 for micro-notched specimens with two different √area (221 and 631 μm), the criteria predictions of the fatigue near threshold behaviour are not fairly good.

Table 1. Summary of mutiaxial fatigue criteria applied

Findley [17]	$\left(\varphi^*,\theta^*\right):\ \max_{(\varphi,\theta)}\left[\tau_a\left(\varphi,\theta\right)+\kappa_F\sigma_{n,max}\left(\varphi,\theta\right)\right]\quad \sigma_{eq}=\tau_a\left(\varphi^*,\theta^*\right)+\kappa_F\sigma_{n,max}\left(\varphi^*,\theta^*\right)\le\sigma_{lim}$
Matake [18]	$\left(\varphi^*,\theta^*\right):\ \max_{(\varphi,\theta)}\tau_a\left(\varphi,\theta\right)$ $\sigma_{eq}=\tau_a\left(\varphi^*,\theta^*\right)+\kappa_M\sigma_{n,max}\left(\varphi^*,\theta^*\right)\le\sigma_{lim}$
Susmel-Lazzarin [19]	$\left(\varphi^*,\theta^*\right):\ \max_{(\varphi,\theta)}\tau_a\left(\varphi,\theta\right)$ $\sigma_{eq}=\tau_a\left(\varphi^*,\theta^*\right)+\kappa_{SL}\dfrac{\sigma_{n,max}\left(\varphi^*,\theta^*\right)}{\tau_a\left(\varphi^*,\theta^*\right)}\le\sigma_{lim}$
Dang Van [20]	$\sigma_{eq}=\max_t\left(\tau_{DV}\left(t\right)+\kappa_{DV}\sigma_H\left(t\right)\right)\le\sigma_{lim}$
Liu-Mahadaven [21]	$\left(\varphi^*,\theta^*\right):\ \max_{(\varphi,\theta)}\sigma_{n,a}\left(\varphi,\theta\right)$ $\sigma_{eq}=\sqrt{\left(\dfrac{\sigma_{n,a}\left(\phi^*,\theta^*\right)}{\sigma_w}\right)^2+\left(\dfrac{\tau_a\left(\phi^*,\theta^*\right)}{\tau_w}\right)^2+\kappa_{LM}\left(\dfrac{\sigma_{h,a}\left(\phi^*,\theta^*\right)}{\sigma_w}\right)^2}\le\sigma_{lim}$
Liu-Zenner [22]	$\sigma_{eq}=\left\{\dfrac{15}{8\pi}\int_0^{\pi}\int_0^{2\pi}\left[a\tau_a^2\left(1+m\tau_m^2\right)+b\sigma_a^2\left(1+n\sigma_m^2\right)\right]\sin\theta d\theta d\varphi\right\}^{\frac{1}{2}}\le\sigma_{lim}$
Papadopoulos [23]	$\sigma_{eq}=\sqrt{\dfrac{5}{8\pi^2}\int_{\varphi=0}^{2\pi}\int_{\theta=0}^{\pi}\int_{\chi=0}^{2\pi}T_a^2\left(\varphi,\theta,\chi\right)d\chi\sin\theta d\theta d\varphi}+\kappa_P\sigma_{H,max}\le\sigma_{lim}$

From data of figure 11, it can be assessed that the critical plane type criteria (Matake, Susmel and Dang Van criteria) strongly underestimate the fatigue threshold since their predictions lie under the experimental material fatigue strength (i.e. negative percentage errors); in particular in the case of the gear steel, prediction errors are always greater than 40% and sometimes they can be greater than 60%. The Papadopoulos criterion gives fairly good predictions of the near threshold behaviour of the bearing steel. Finally, the Liu-Mahadaven criterion is not consistent, it only gives a correct prediction in the case of gear steel micro-notched specimen with defect √area of 221 μm.

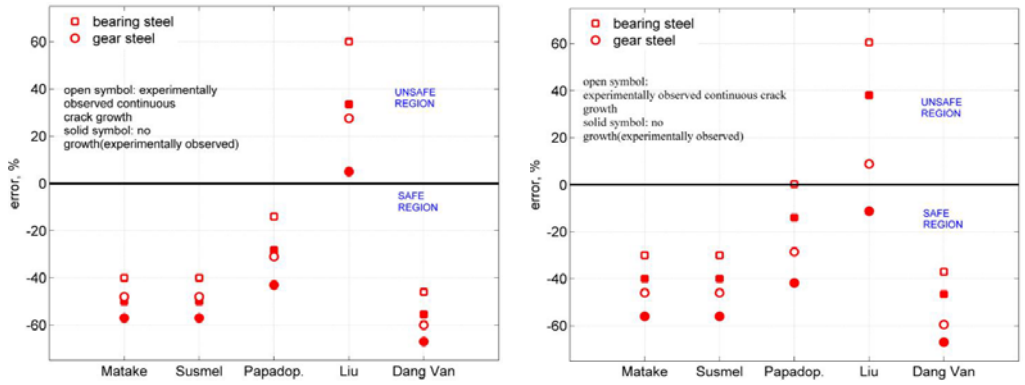

Figure 11. Prediction percentage errors of the fatigue near threshold behaviour of micro-notched specimens: a) √area=631 μm; b) √area=221 μm

Surface rubbing : estimation of cyclic plastic zone

The enhanced propagation under out of phase tests does not appear to be justified within a "LEFM description". In fact the superposition of compression onto an alternating shear leads to an increase of dissipation with a reduction of crack driving force [1,16, 24] respect to simple shear. On the other hand if we considered friction on the crack faces together with the opening of the crack flanks due to rubbing, the "enhanced" shear propagation respect to simple torsion can be explained. FE analysis of crack driving force are currently confirming this intuitive explanation.

Surface rubbing : estimation of cyclic plastic zone

As previously mentioned the out-of-phase loading promotes Mode III co-planar crack growth in comparison with pure torsion. The crack rubbing/deformation could promote shear propagation since it prevents the friction of the crack faces.

In order to explain this behaviour, the plastic zones radius has been calculated. An estimation of the size and the shape of the plastic zone at the bottom of the micro notches can be made by substituting the singular stress field [25] at the crack tip in the Von Mises yield criterion, and solved for the maximum plastic zone radius r_P.

This procedure has been applied, for both the out-of-phase loading path and the pure torsional loading path, considering a small 20 μm crack at the bottom of the micro notches (the Mode I pre-crack), where K_{II} is approximately equal to zero. In the case of the OOP loading scheme the plastic zone has been estimated by computing the maximum plastic radius during the loading cycle for every direction around the crack front under the hypothesis that the permanent deformation of crack lips allows compression at the crack tip.

Sketches of the plastic zone shapes are shown in Figure 12 for gear steel material micro-notched specimens with defect area √221 μm tested at two different stress ratios $\Delta K_{III} / \Delta K_{I,th} = 1.08$ and $\Delta K_{III} / \Delta K_{I,th} = 0.45$. The plastic zone sizes under both mixed mode I+III and under pure torsion have been compared.

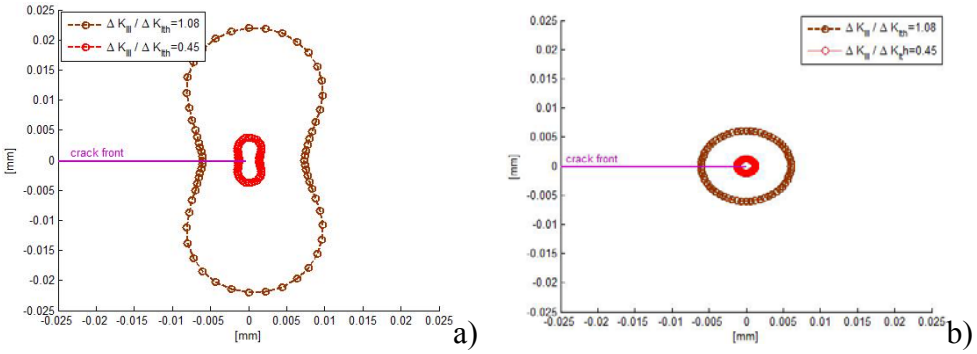

Figure 12. Plastic zone shapes for gear steel material micro-notched specimens with defect area √221 μm at two ratios $\Delta K_{III} / \Delta K_{I,th}$: a) mixed-mode I+III; b) pure mode III

It can be observed from Figure 12 that the superimposed compression results in a plastic zone extent which is almost three time the one obtained under pure torsion. Moreover, the plastic extent is strongly reduced in correspondence of the near threshold value of the applied $\Delta K_{III} / \Delta K_{I,th}$.

CONCLUSIONS

A new experimental method has been developed in order to promote mode III co-planar crack propagation. At this purpose a preliminary Mode I fatigue test pre-cracking procedure has been adopted.

Multiaxial fatigue tests have been carried out both on a gear and a bearing steel material micro-notched specimens. Three defect sizes, expressed in terms of Murakami's √area parameter, equal to 631 μm, 314 μm and 221 μm have been considered. In order to simulate the real state of stress in rolling contact fatigue problems, the adopted loading path was characterized by an axial force always in compression and shifted on 90° degrees relatively to the torsional cycle.

All OOP fatigue tests showed predominant shear coplanar Mode III propagation in comparison with a relatively small or absent surface propagation.

The results for two different steels showed that the presence of a superimposed compression enhanced the shear coplanar growth resulting in $\Delta K_{th,III}$ values much lower than the threshold condition for simple torsion. This enhanced damage mechanism, that cannot be described neither in terms of fatigue criteria nor in terms of crack driving force at the crack tip, was characterized by intense plastic deformation and rubbing of crack lips with an opening of the crack faces.

REFERENCES

[1] Murakami Y, Fukushima Y, Toyama K, Matsuoka S. *Fatigue crack path and threshold in Mode II and Mode III loadings*. Engineering Fracture Mechanics; 2008; 75:306-318.

[2] Donzella G, Petrogalli C, *A failure assessment diagram for components subjected to rolling contact loading*. International Journal of Fatigue; 2010; 32: 256-268.
[3] Pokluda J. Slamecka K. Sandera P. *On the mechanism of factory-roof formation*. Crack Paths 2009, Vicenza.
[4] Tschegg E.K, *A contribution to mode III fatigue crack propagation*. Material Science end Engineering; 1982; 54: 127-136.
[5] Nayeb-Hashemi H, Mcclintock F.A, Ritchie R.O, *Micro-mechanical modelling of mode III fatigue crack growth in rotor steel*. International Journal of Fracture; 1983; 23:163-185.
[6] Murakami Y, Takahashi K, Kusumoto R, *Threshold and growth mechanism of fatigue cracks under mode II and mode III loading*. Fatigue Fract Engng Mater Struct; 2003; 26: 523-531
[7] Pokluda J, Pippan R, *Can pure mode III fatigue loading contribute to crack propagation in metallic materials?* Fatigue Fract Engng Mater Struct; 2008; 28: 179-185
[8] Guy P, Meynaud P, Vincent A, Dudragne G, Baudry G, Sub-surface damage investigation by high frequency ultrasonic echography on 100Cr6 bearing steel. Tribology International; 1997; 30: 247-259
[9] Vincent A, Lormand G, Lamagnere P, Gosset L, Girodin D, Dudragne G, Fougeres R, *From white etching areas formed around inclusions to crack nucleation in bearing steels under rolling contact fatigue*. Bearing Steel STP 1327: 108-123.
[10] K.L. Johnson, *Contact Mechanics*, Cambridge University Press, Cambridge, 1985.
[11] Beretta S, Foletti S, Valiullin K. *Fatigue strength for shallow defects/cracks in torsion*. International Journal of Fatigue; 2010; submitted
[12] S. Beretta, S. Foletti, K. Valiullin, *Fatigue crack propagation and threshold under out-of-phase mutiaxial loading in a gear steel*, submitted to Eng. Fract. Mech
[13] Pinna C, Doquet V. *The preferred fatigue crack propagation mode in a M250 maraging steel*. Fatigue Fract. Engng. Mater. Struct.; 1999; 22:173-183.
[14] Doquet V, Pommier S. *Fatigue crack growth under non-proportional mixed-mode loading in ferritic-pearlitic steel*. Fatigue & Fracture of Engineering Materials & Structures; 2004; 27:1051-1060.
[15] Otsuka A, Fujii Y, Maeda K. *A new testing method to obtain mode II fatigue crack growth characteristics of hard materials*. Fatigue & Fracture of Engineering Materials & Structures; 2004; 27:203-212.
[16] Melin S. *When does a crack grow under mode II conditions?* International Journal of Fatigue; 1986; 20:103-114.
[17] Findley WN, *A theory for the effect of mean stress on fatigue of metals under combined torsion and axial load or bending*, J Engng Industry; 1959; 81: 301–306.
[18] Matake T, *An explanation on fatigue limit under combined stress*. Bull JSME**;** 1977; 20:257–263.
[19] Susmel L, P Lazzarin, A *bi-parametric Wöhler curve for high cycle multiaxial fatigue assessment,* Fatigue Fract Engng Mater Struct; 2002; 25: 63-78.
[20] K. Dang Van, *Macro–micro approach in high-cycle multiaxial fatigue*. In: D.L. McDowell and R. Ellis, Editors, Advances in Multiaxial Fatigue, ASTM STP 1191, Philadelphia (1993), pp. 120–130
[21] Liu Y, Mahadevan S, Threshold stress intensity factor and crack growth rate prediction under mixed-mode loading, Engineering Fracture Mechanics; 2007; 74: 332-345.
[22] Zenner, R.Heidenreich, I.Richter, *Dauerschwingfestigkeit bei nichtsynchroner mehrachsiger Beanspruchung.* Z. Werkstoffiech; 1985; 16: 101–112.
[23] Papadopoulos IV. *Fatigue limit of metals under multiaxial stress conditions: the microscopic approach*. Technical note no. 1.93.10 1, ISEI/IE 2495/93. Commission of the European Communities, Joint Research Centre; 1993.
[24] Valiullin K. *Multiaxial fatigue in the presence of defects*. Ph.D. thesis. Politecnico di Milano, 2010.
[25] Richard HA, Fulland M, and Sander M. *Theoretical crack path prediction*. Fat. Fract. Engng. Mater. Struct.; 2005; 28:3-12.